INSTITUTE OF PHYSICS PUBLISHING PLASMA SOURCES SCIENCE AND TECHNOLOGY

Plasma Sources Sci. Technol. **14** (2005) S1–S8 doi:10.1088/0963-0252/14/2/S01

He_2^+ molecular ions in helium glow discharges: the effect of bulk electron temperature

Kinga Kutasi[1], **Péter Hartmann, Gergely Bánó and Zoltán Donkó**

Research Institute for Solid State Physics and Optics, Hungarian Academy of Sciences, POB 49, H-1525 Budapest, Hungary

E-mail: kutasi@sunserv.kfki.hu

Received 23 September 2004, in final form 9 February 2005
Published 4 May 2005
Online at stacks.iop.org/PSST/14/S1

Abstract

He_2^+ molecular ions may be present in a concentration comparable to that of atomic ions in dc helium glow discharges operated at medium pressures (several tens of millibars). We use hybrid discharge simulations to study in a self-consistent way the creation, transport and loss processes of both atomic and molecular ionic species and the role of molecular ions in the self-sustainment of the discharges. In the pressure range where recombination processes are significant, the temperature of the cold (bulk, trapped) electrons is expected to strongly influence the discharge properties. In order to clarify these effects we investigate the influence of cold electron temperature (used as an input parameter) on the results of the simulations based on a hybrid model.

1. Introduction

Noble gas (among them helium) discharges operated at elevated pressures [1, 2] are attractive sources of radiation in a wide spectral range; their applications range from lasers [3, 4], through different types of lamps [5], to plasma addressed liquid crystal displays [6]. The UV and VUV radiation of helium discharges originate from the excited He_2 and He_2^+ molecules. As the ground state of the He_2 molecule is unstable, excited He_2 molecules result mainly from the recombination of He_2^+ ions. In order to optimize their applications, an understanding of the processes taking place in such discharges is of primary importance [7, 8].

We choose the technique of hybrid modelling as a tool for our theoretical investigations into negative glow He discharges. Hybrid models have successfully been applied during the last decade for self-consistent simulation of dc and RF as well as transient glow discharges [9–14]. In the case of low-pressure noble gases, these models are usually based on a two-component fluid approach (for positive ions and slow electrons), and use Monte Carlo (MC) simulation of fast electrons to calculate the ionization source in an accurate manner. The partitioning of the electrons into groups of fast and slow (bulk) electrons makes the solution of the problem computationally efficient. The fast electrons are treated at the kinetic level, and at the moment when they are no longer able to produce any excitation and ionization of the gas, they are transferred to the slow electron group. As a simplification, hybrid models of negative glow discharges conventionally use a constant characteristic energy for the slow electrons, e.g. [10–12], which is chosen to be $kT_e = 1$ eV in almost all studies. Using experimentally determined values of T_e, one could increase the reliability of the results of such calculations. At certain discharge conditions (depending on the gas pressure, charge density, probe dimensions, etc) Langmuir probe measurements can be used to determine T_e [15]. At high pressures the partial local thermodynamic equilibrium (PLTE) also makes it possible to determine the electron temperature from the intensity ratio of a sequence of spectral lines [16]. In some previous investigations on low-pressure negative glow discharges, cold electron temperatures significantly lower than 1 eV have been found. These studies include the laser based diagnostics of Den Hartog *et al* [17], theoretical calculations of Arslanbekov and Kudryavtsev [18], Langmuir probe measurement of Bogaerts *et al* [19], Angstadt *et al* [20] and Ohsawa *et al* [21], Thomson scattering measurements of Gamez *et al* [22] and experimental investigations of hollow cathode discharges by Warner [23], Leigh [24] and Bánó *et al* [25]. In all these works cold

[1] Author to whom any correspondence should be addressed.

electron temperatures ranging between 0.08 and 0.5 eV have been found. Considering these data, the 1 eV value, used in most hybrid model-based simulations, may be too high. To the best of our knowledge no previous study addressed the question 'how do the results of such calculations depend on the T_e value assumed in the simulations?' This question may be even more important when the gas pressure (and charge densities) reaches a threshold when recombination processes—whose rates depend very strongly on T_e—become essential in the particle balance. Thus we feel it is justified and timely to explore this effect in a wide pressure range.

The aims of our work are (i) to investigate the characteristics of helium glow discharges including molecular ions through hybrid simulations; (ii) to study the effect of different elementary processes on the discharge characteristics; and (iii) to determine the role of molecular ions in the self-sustainment of helium discharges in a wide pressure range. Compared with our earlier studies [26], the present discharge model is expected to be more accurate as the dissociative recombination process is also taken into account in addition to other recombination channels. The spectroscopic determination of the bulk electron temperature—based on the not fully justified PLTE approximation for the investigated discharge conditions [26]—is replaced by Langmuir probe measurements. Unfortunately these measurements cannot cover the entire pressure range considered here. Thus in most of our simulations we study the effect of the assumed T_e on the calculated discharge characteristics, rather than using experimentally determined bulk electron temperature values.

In our work we investigate similar glow discharges in the 2–60 mbar pressure range. Four different discharges are studied at the conditions which correspond to the same $pL = 6\,\text{mbar cm}$ and reduced current density $j/p^2 = 0.027\,\text{mA cm}^{-2}\,\text{mbar}^{-2}$: (i) $p = 2\,\text{mbar}$, $j = 0.108\,\text{mA cm}^{-2}$, $L = 3\,\text{cm}$, (ii) $p = 6\,\text{mbar}$, $j = 0.972\,\text{mA cm}^{-2}$, $L = 1\,\text{cm}$, (iii) $p = 20\,\text{mbar}$, $j = 10.8\,\text{mA cm}^{-2}$, $L = 0.3\,\text{cm}$ and (iv) $p = 60\,\text{mbar}$, $j = 97.2\,\text{mA cm}^{-2}$, $L = 0.1\,\text{cm}$.

This paper is divided into five sections. Section 2 describes the experimental arrangement and experimental results. In section 3 the self-consistent model is described. The modelling results are presented and discussed in section 4. The summary of the work is given in section 5.

2. Experimental

Our earlier experimental investigations [26]—where the electrical characteristics and the optical emission spectra of similar helium glow discharges in the 6–60 mbar pressure range have been measured—are complemented with the measurement of the electron temperature by probe measurements at low pressures. For the discharge conditions given above (including our previous [26] and present experimental studies), the discharge voltage is $V = 350 \pm 10\,\text{V}$ over the whole pressure range, i.e. the $V = f(j/p^2)$ scaling is found to be fulfilled within the limit of errors. For the present measurements we use a plane-parallel electrode configuration: two copper discs of 7.8 cm diameter placed in a glass tube face each other at a distance of 3 cm. This construction has been mounted inside a vacuum chamber evacuated by a turbomolecular pump backed by a rotary pump. The base pressure of the system is $\sim 5 \times 10^{-7}\,\text{mbar}$. During the course of measurements a gas flow of 1 sccm of 6.0 purity He gas is established through the chamber.

It is well known that the transition part of the Langmuir probe characteristics (where the probe voltage is higher than the floating potential and lower than the plasma potential and the ion current is negligible) can be used for determination of the temperature of Maxwellian bulk electrons. The electron temperature can be obtained fitting the exponential part of the probe characteristic in this region. The inverse slope of the semilogarithmic plot of the probe current versus voltage is proportional to kT_e. This slope is insensitive to the shape of the probe and collisions in the probe sheath [15]. The problems related to the contamination of the Langmuir type (cold) probes can be overcome with heated probes operated below the electron emission threshold. We have constructed such a probe using 0.07 mm tungsten wire of $\approx$4 mm length. The tungsten wire is mounted between two glass tubes of $\approx$1 mm diameter and 5 mm length, joined with a 2.4 mm diameter ceramic tube with two holes (see the sketch of the probe in the inset of figure 1). The probe is introduced into the discharge volume through a hole in the anode and can be positioned by a micrometer screw equipped with vacuum feed-through.

The probe characteristics have been recorded for different heating currents (I_h) and have been found to become reproducible above certain values of I_h. In order to eliminate the errors originating from the finite value of voltage drop over the length of the probe (which is of the order of $\approx$1 V), the data have been taken during short time intervals (typically 100 μs) when the heating is interrupted. The heating current has been kept low, so that no evidence of emitted electrons has been observed.

A typical probe characteristic taken at $p = 2\,\text{mbar}$ pressure and $I = 5\,\text{mA}$ discharge current is plotted in figure 1. The characteristic has been recorded at the position of the maximum charge densities (1.50 cm from the cathode for the above discharge conditions), which has been found by maximizing the electron current to the probe at a fixed value of positive probe bias (+18 V). We made no attempt to determine the absolute values of charge densities from the

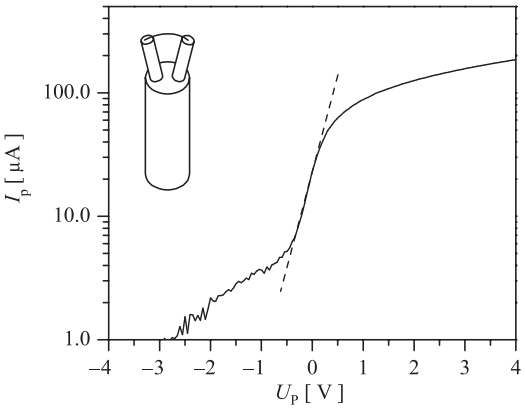

Figure 1. Probe characteristic recorded at $p = 2\,\text{mbar}$ at $x = 1.5\,\text{cm}$ from the cathode, corresponding to the position of the maximum density in the negative glow. The discharge voltage is $U = 350\,\text{V}$, the reduced current density is $j/p^2 = 0.027\,\text{mA cm}^{-2}\,\text{mbar}^{-2}$. The dashed line is a linear fit to the characteristic. The inset of the figure shows a sketch of the probe.

probe characteristics. The semilogarithmic plot of the probe current versus voltage clearly contains a linear part, i.e. there exists a population of the electrons with nearly Maxwellian energy distribution. The inverse slope defines the electron temperature (according to $I_e = I_{es} \exp[e(V_p - V_s)/kT_e]$), which in the case plotted in figure 1 amounts to $kT_e = 0.28$ eV. There is also a clear indication of the presence of high-energy electrons, as is expected in the negative glow. Due to this fact the electron temperature obtained by fitting the exponential part of the probe characteristic may be slightly overestimated.

Determination of the electron temperature at higher pressures using the probe technique was not feasible mostly due to technical difficulties. At higher pressures, due to the *pd* scaling the discharge dimensions are reduced, e.g. giving an electrode separation of only 0.3 cm at 20 mbar. The possibility of reduction of the probe dimensions is limited; the available probe construction does not fit the narrow discharge gap at high pressures. Therefore—as stated in the introduction—the effect of the kT_e value assumed in the model on the calculated discharge characteristics is studied for a wide pressure range.

3. Simulation model

The discharge is described by a one-dimensional hybrid model which combines

- a fluid model for atomic and molecular ions and slow electrons
- MC simulation of fast electrons and
- a diffusion–reaction model of the metastable species.

The model makes it possible to calculate several discharge characteristics in a self-consistent way. The elementary processes taken into account in the model are summarized in table 1: for a more detailed discussion see [26]. Here we only briefly summarize the features of our model—for more details the reader is referred to [26].

For fast electrons we take into account elastic scattering (p1), excitation to metastable and several higher excited states (up to $n = 5$) (p2–p3) as well as ionization (p4) (the cross section data are taken from [27]). The excited atoms (including the $n = 3$ to $n = 5$ states) can participate in associative ionization process (p5) in which molecular ions are created [28]. The singlet and triplet atomic metastables may be converted into triplet atomic and molecular metastables, respectively (p6–p7). The singlet atomic metastables may also be converted to ground state atoms due to collisions with the gas atoms (p8). The atomic and molecular ions are partly created in metastable–metastable associative ionization processes which result in the loss of metastables (p9). The metastables are also lost in deexcitation processes (p10–p11) [29]. The atomic ions convert into molecular ions through the ion conversion process (p12) [29]. The atomic ions are lost through collisional radiative (p13) [29] and radiative recombination (p14) [30]. The molecular ions are lost through dissociative recombination (p15) [31] (this process was not taken into account in the model of [26]), collisional radiative recombination (p16) [30] and three-body recombination (p17) processes [29].

Table 1. Elementary processes considered in the model.

Proc. id.	Reaction process
p1	$He + e^- \rightarrow He + e^-$
p2	$He + e^- \rightarrow He(S, T) + e^-$
p3	$He + e^- \rightarrow He^* + e^-$
p4	$He + e^- \rightarrow He^+ + 2e^-$
p5	$He^* + He \rightarrow He_2^+ + e^-$
p6	$He(S) + e^- \rightarrow He(T) + e^-$
p7	$He(T) + 2He \rightarrow He(M) + He$
p8	$He(S) + He \rightarrow 2He$
p9	$He(S, T) + He(S, T) \rightarrow He^+ + He + e^-$ $He_2^+ + e^-$
p10	$He(S) + e^- \rightarrow He + e^-$
p11	$He(T) + e^- \rightarrow He + e^-$
p12	$He^+ + 2He \rightarrow He_2^+ + He$
p13	$He^+ + 2e^- \rightarrow He^* + e^-$
p14	$He^+ + e^- \rightarrow He + h\nu$
p15	$He_2^+ + e \rightarrow He(1\,^1S) + He(2\,^3S)$
p16	$He_2^+ + 2e^- \rightarrow He_2^* + e^-$
p17	$He_2^+ + e^- + He \rightarrow He_2^* + He$

He(S), He(T) and He(M) denote the singlet atomic, triplet atomic and molecular metastables, respectively. For more details see [26].

In the simulation the fluid, MC and metastable models are solved in an iterative way until the stationary state of the discharge is reached. The structure of the hybrid model and the transfer of physical quantities between the three models are presented on the flowchart shown in figure 2. In the first step of the iterations the fluid model is solved without sources and losses of charged particles to obtain an 'initial' electric field distribution, and the avalanches initiated by a given number of primary electrons are traced afterwards by the MC simulation in this field. Using the metastable source functions calculated in the MC cycle, the metastable model is solved to obtain the sources of the atomic and molecular ions created in the metastable–metastable associative ionization processes. In the metastable–metastable associative ionization processes fast electrons are also created. These electrons are traced in the next MC cycle. In the next step the fluid model is solved using the ion and electron sources and losses obtained in the MC and metastable cycles.

The typical integration time step in the fluid model is of the order of 1 ns; the MC and metastable parts are usually run after 100 steps in the fluid model. Typically 1000 primary electrons and their secondaries are traced in the MC procedure. Having obtained the converged solution, the MC simulation is carried out once more for 2×10^5 primary electrons to obtain sufficiently smooth source functions.

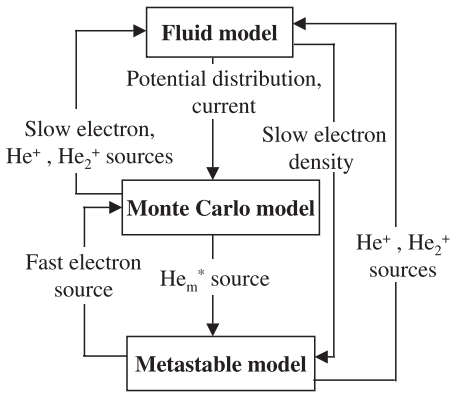

Figure 2. Flowchart of the model.

The input parameters of such a hybrid model are the discharge voltage, gas pressure, rate coefficients of different processes, electron collisional cross sections, diffusion and mobility coefficients, temperature of bulk (slow) electrons (kT_e) and the secondary electron emission coefficient (γ). One part of these parameters can be determined experimentally, and the other part can be found in the literature; however, there is a lack of data for the (i) electron temperature and (ii) secondary electron emission coefficient.

The importance of the electron temperature has been discussed in the introduction part. Besides the electron temperature another critical parameter of hybrid models is the secondary electron emission coefficient, γ. Data for γ in the literature can be found mainly from high vacuum beam experiments using clean electrode surfaces. Such data for γ cannot be directly used in discharge modelling [36]. In hybrid models there is a trend to use a constant γ for different discharge conditions. Previous studies have, however, shown that the effective secondary electron emission coefficient (the ratio of the electron current to the ion current at the cathode) depends on the reduced electric field (E/n) at the cathode [32–35]. The effective γ coefficient accounts for all possible electron emission mechanisms [36]. In our model the electron emission is attributed to the atomic and molecular ions. The secondary yield of He_2^+ ions is expected to be about 60% of He^+ [37, 38]. In this way the discharge current is $I = I_{He^+ + He_2^+} + \gamma_{He^+}(I_{He^+} + 0.6 I_{He_2^+})$. To have a correct description of the discharges the secondary yield of atomic ions, γ_{He^+}, needs to be chosen carefully. γ_{He^+}, in fact, can be determined in the hybrid model by taking it as a variable parameter and in the iterative solution of the model (at fixed discharge voltage) adjusting it in a way so as to obtain a current density equal to the experimental value [39].

Calculation of the heating of the gas is not included in our model. This is justified by the rather moderate values of E/n in the cathode sheath (see later) not allowing the creation of a significant amount of fast neutral atoms (in charge and momentum transfer collisions between positive ions and the background gas) which would be the dominant species heating the gas through their collisions with background He atoms.

4. Results and discussion

First the results of the 'base simulations' carried out for a 2 mbar pressure are presented. For this case the experimentally determined $kT_e = 0.28$ eV bulk electron temperature is used as input data, and the procedure explained above is used for determination of the effective electron yield. The results show that for this case the agreement between the measured and calculated current densities is reached at $\gamma_{He^+} = 0.109$ and $\gamma_{He_2^+} = 0.065$. For these conditions the reduced electric field at the cathode $(E/n)_c$ is found to be 1800 Td. Our γ_{He^+} value agrees well with that given in [40]. As we investigate similar discharges where the reduced electric field at the cathode is constant, the use of the same γ_{He^+} value (obtained in the way described earlier) for the calculations at higher pressures (keeping pd and j/p^2 constant) is reasonable.

The charge density distributions—shown in figure 3(*a*)—indicate the presence of a quasi-neutral plasma in the negative glow and the dominance of the positive ions in the cathode

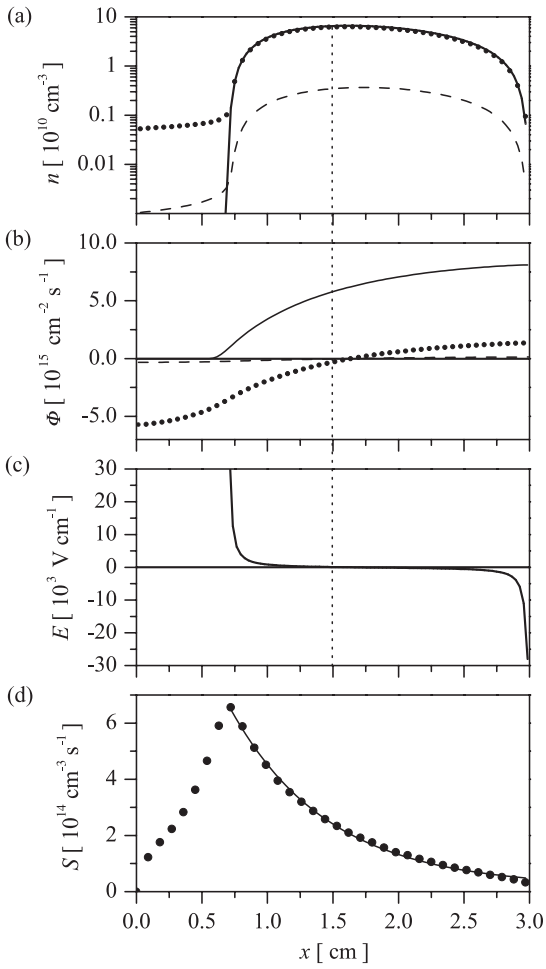

Figure 3. (*a*) Density distribution of the slow electrons (——) and atomic (●) and molecular (– – –) ions. (*b*) Flux of the slow electrons (——) and atomic (●) and molecular (– – –) ions. (*c*) Axial distribution of the electric field in the negative glow. (*d*) Axial distribution of the calculated electron ionization rate (●). The solid line is a single exponential decay curve fitted to the data.

sheath. According to the calculated charge fluxes (figure 3(*b*)) a part of the ions flow to the anode, which is the consequence of the small negative field present in the anode vicinity, due to the reversal of the electric field in the negative glow [41], see figure 3(*c*). The modelling results show that—for the above discharge conditions—the position of the field reversal is located at $x \cong 1.60$ cm (from the cathode) and coincides with the position of the maximum density. In the probe measurements for the position of the maximum density we found 1.50 cm, which is in very good agreement with the modelling result. The position of the field reversal can also be calculated with a formula given by Bouef and Pitchford [41]. According to their analytical model the position of the field reversal, d_f, depends only on the electrode distance, d, the length of the cathode sheath, d_c, and the energy relaxation length of the fast electrons, λ:

$$\frac{d_f - d_c}{d - d_c} = -\Lambda \ln[\Lambda(1 - e^{-1/\Lambda})], \qquad (1)$$

where $\Lambda = \lambda/(d - d_c)$. The energy relaxation length of the electrons has been determined from the decay of the calculated

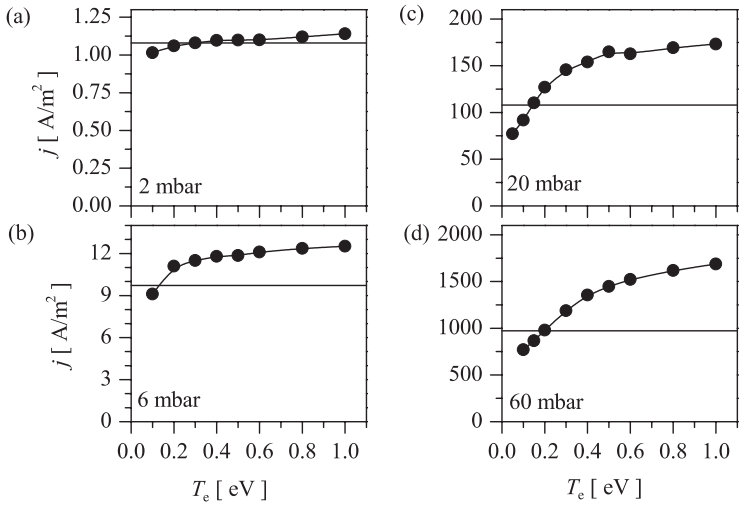

Figure 4. Calculated current density (●) as a function of the assumed electron temperature at different gas pressures. The heavy horizontal lines in the panels represent the experimental current density at $U = 350$ V.

ionization rate beyond the peak of the ionization source in the negative glow (figure 3(*d*)). The position of the cathode sheath edge coincides with the position of the ionization source peak [33]. Following this procedure the position of the field reversal is found from equation (1) to be at $d_f = 1.59$ cm. The uncertainty of the experimental determination of the position of the maximum electron density can be estimated to be within ≈0.1–0.2 cm. This uncertainty is due to the flat electron density profile in the middle of the negative glow region, which results only in a slight change in the electron current of the probe with position (at a constant positive bias, e.g. +18 V). In the determination of d_f from equation (1), the sources of errors are (i) the uncertainty of the electron energy relaxation length, which is calculated from the ionization source function (supposed to have an exponential decay) and (ii) the uncertainty of the determination of the length of the cathode sheath. The uncertainty of the value given by equation (1) is thus estimated to be ⩽10%.

As we discussed in the introduction, the dependence of the calculated discharge characteristics on the assumed value of the electron temperature is studied in detail in the forthcoming part of this paper. First the dependence of the current density on kT_e at different pressures is studied. The results are illustrated in figure 4: the current density increases with increasing electron temperature. The results show that in order to obtain by modelling the experimental current density the electron temperature in the discharges of 6–60 mbar pressure has to be chosen in the 0.1–0.2 eV range. This is in reasonable agreement with our previous measurements, based on spectroscopical observations [26], where kT_e values in the 0.1–0.12 eV range have been obtained. It is noted, however, that for these conditions the PLTE requirement, needed for spectroscopical measurements, is not strictly satisfied. The deviation from the thermodynamic equilibrium causes errors in the electron temperature determination from the spectroscopical data. Assuming higher kT_e values in the hybrid models, the current density can be strongly overestimated. At low pressures, assuming an electron temperature of 1 eV introduces a 20% error in the current density; however, with increasing pressure this error increases and at 60 mbar reaches 60%. This strong dependence of the current densities on the electron temperature let us conclude that for correct modelling, accurate determination of the electron temperature is required.

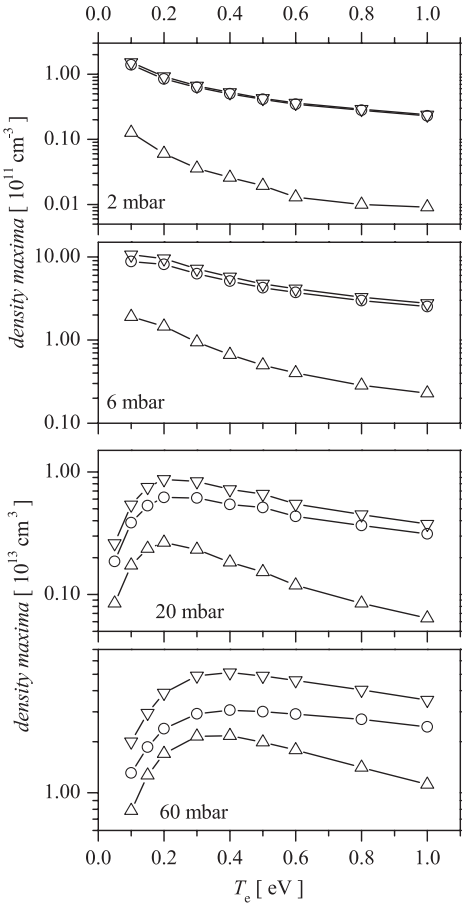

Figure 5. Maxima of electron (▽), atomic ion (○) and molecular ion (△) densities as a function of the assumed electron temperature at different gas pressures.

In the following, the dependence of the calculated charge densities on the bulk electron temperature assumed in the model is investigated. Figure 5 shows the maximum values

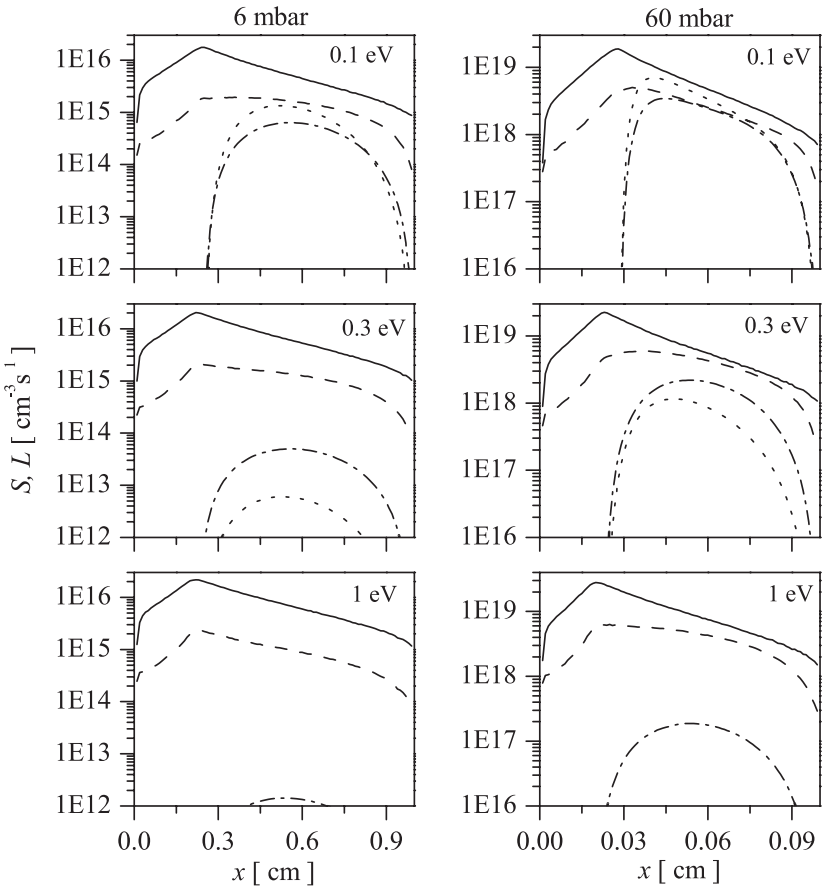

Figure 6. Source functions of atomic (——) and molecular (– – –) ions, and recombination loss functions of atomic (· · · · · ·) and molecular (— · —) ions at 6 mbar and 60 mbar pressure for different assumed values of the electron temperature.

of charge densities as a function of the assumed kT_e. At low pressures (2–6 mbar) we can observe the expected behaviour of the charge densities, namely the decrease in the density with increasing electron temperature. This behaviour can be explained by the increase in the electron diffusion coefficient resulting in the increase of the ambipolar diffusion. At higher pressures the densities show maxima as a function of the electron temperature at around 0.2–0.3 eV. The decrease in densities towards lower kT_e is due to the additional loss of charges due to recombination processes at high pressures, in contrast with low-pressure cases, where the recombination losses are less important. Figure 6 displays the source (S) and recombination loss (L) functions of atomic and molecular ions for 6 and 60 mbar pressures, for 0.1, 0.3 and 1 eV electron temperatures. Assuming a 0.1 eV electron temperature at 6 mbar, 9% of ions (7% of atomic and 20% of molecular ions) recombine, while at 60 mbar 36% (30% of atomic and 52% of molecular ions) do so. The rest of the ions are lost at the electrode surfaces. The recombination losses decrease with increasing electron temperature: for $kT_e = 0.3$ eV at 6 mbar the recombination is already negligible (only 2% of molecular ions recombine), while at 60 mbar 11% of the ions recombine (5% of atomic and 25% of molecular ions). In the case of 1 eV electron temperature, recombination becomes negligible even at 60 mbar, where 2% of molecular ions recombine. This low recombination rate at 60 mbar cannot explain the presence of strong molecular bands in the experimental optical emission spectra presented in our earlier work [26]. This result also supports the observation that the bulk electron temperature in helium glow discharges is much lower than 1 eV.

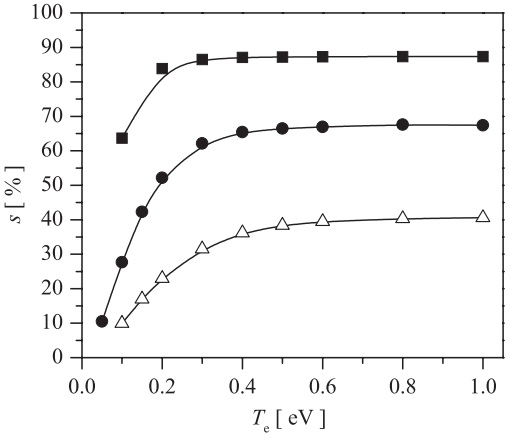

Figure 7. The ratio of the dissociative recombination losses and the total recombination losses for the molecular ions as a function of the assumed electron temperature for 6 mbar (■), 20 mbar (●), 60 mbar (△).

The relative importance of different recombination processes has been investigated using the model. Here we wish to emphasize the importance of the dissociative recombination process, which is a new process included in the model compared with the model presented in [26]. Figure 7 shows

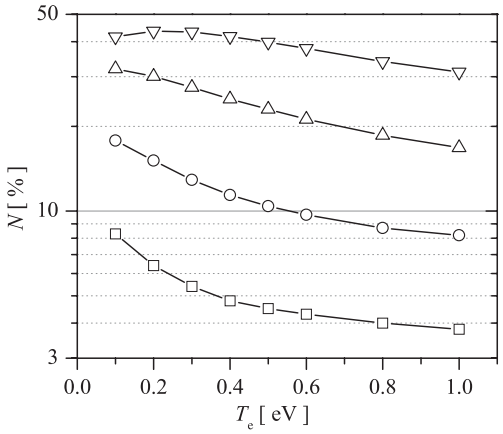

Figure 8. Percentage of molecular ions in the negative glow as a function of the assumed electron temperature at 2 mbar (□), 6 mbar (○), 20 mbar (△), 60 mbar (▽).

the ratio of the dissociative recombination loss to the total recombination loss of the molecular ions as a function of the assumed electron temperature. At the highest pressure investigated, 60 mbar, at 0.2–0.3 eV electron temperature the dissociative recombination has a share of 20–30% of the total loss by recombination; this percentage increases with decreasing pressure—at 20 mbar it is around 50–60% and at 6 mbar it increases to 85%.

The electric field distribution in the discharge is determined by the charge density distributions. In the negative glow, which is an almost field-free region, a quasi-neutral plasma is present composed of atomic and molecular ions and slow (bulk) electrons. In the following the percentage of molecular ions in the negative glow as a function of the assumed kT_e is studied and presented in figure 8. The percentage of molecular ions decreases with increasing electron temperature; in comparison with the 0.1 eV case, at 1 eV the percentage of molecular ions decreases by about 10% at $p = 60$ mbar. The results show that in the 0.1–0.3 eV range, the percentage of molecular ions decreases by about 5% in the case of 2, 6 and 20 mbar, while at 60 mbar it increases by about 2%. In the case of $kT_e = 0.3$ eV—which is supposed by us to be a realistic value for the electron temperature—at 2 mbar 5% of ions are molecular ions, at 6 mbar 12%, at 20 mbar 28% and at the highest pressure investigated (60 mbar) 42%.

The percentage of the ion current carried by molecular ions at the cathode as a function of the assumed electron temperature is presented in figure 9(*a*). The ratio of the molecular ion current, $I_{He_2^+}$, to the total ion current shows a slight dependence on the electron temperature. In the case of $kT_e = 0.3$ eV at 2 mbar 5% of the ion current is carried by the molecular ions, and at 6 mbar this percentage increases up to 12% and at 60 mbar reaches 25%. The self-sustained mode of operation of the discharge is assured by the ions arriving at the cathode surface which induce the emission of secondary electrons. Figure 9(*b*) shows the percentage of secondary electrons released by the molecular ions, $r = 100 \times \gamma_{He_2^+} I_{He_2^+} / (\gamma_{He_2^+} I_{He_2^+} + \gamma_{He^+} I_{He^+})$. At 2 mbar 3% of the electrons are released by the molecular ions, at 6 mbar 7% and at 60 mbar 17%. These results give us an insight about the increasing importance of molecular ions in the self-sustainment of the discharge.

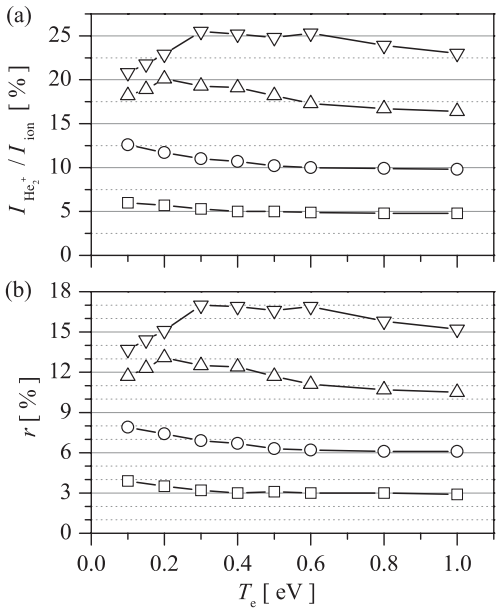

Figure 9. (*a*) Percentage of the ion current carried by the molecular ions at the cathode and (*b*) percentage of secondary electrons released by molecular ions at the cathode as a function of the assumed electron temperature at 2 mbar (□), 6 mbar (○), 20 mbar (△), 60 mbar (▽).

5. Summary

The role of molecular ions in low-pressure negative glow helium discharges has been investigated by means of a hybrid model which combines (i) a fluid description of slow electrons and atomic and molecular ions with (ii) MC simulation of fast electrons and (iii) a diffusion–reaction model for metastable species. The bulk electron temperature (T_e) has been determined experimentally at the lowest pressure studied, 2 mbar, using a (heated) Langmuir probe. This experimentally obtained value, $kT_e = 0.28$ eV, has been used as an input parameter for the 'base simulations' carried out for $p = 2$ mbar, from which—among other discharge characteristics—the secondary electron yield of atomic ions, γ_{He^+}, was also determined.

Subsequently, discharges at pressures up to 60 mbar have been investigated through simulations: these calculations have been carried out for constant values of the pL and j/p^2 similarity parameters, and at a constant discharge voltage $V = 350$ V. Due to the similarity of the discharges studied, γ_{He^+} was also kept constant at the value 0.109 determined at 2 mbar. As the experimental determination of the electron temperature at higher pressures using the probe technique was not feasible, the effect of the kT_e value assumed in the model on the calculated discharge characteristics has been studied. The comparison of the measured and calculated current densities indicated that the electron temperature in the 2–60 mbar pressure domain is in the 0.1–0.3 eV range, which is significantly lower than the $kT_e = 1$ eV value conventionally used in hybrid models. We have shown that by assuming $kT_e = 1$ eV—as the majority of hybrid models do—the current density of the discharges can be significantly overestimated (especially at higher pressures).

At low pressures the maxima of the charge densities decreased with an increase in the assumed value of kT_e, due

to the increasing ambipolar diffusion. At high pressures ($\geqslant$20 mbar)—where recombination processes become very important at low kT_e values—the peak value of the charge density showed a maximum as a function of kT_e.

At 2 mbar the position of the maximum electron density was found to occur at $x = 1.50$ cm from the cathode, while the modelling results gave 1.60 cm, which coincides with the position of the field reversal. The latter has also been determined with the formula given by Bouef and Pitchford [41], and has been found to occur at 1.59 cm. The analysis of the 'composition' of the negative glow plasma showed that at 2 mbar 5% of the ions are molecular ions, and this value increases to 42% at 60 mbar.

Acknowledgments

This work was supported by the Hungarian Science Foundation (Grants OTKA T-34156 and T-48389). We thank K Wiesemann, N Bibinov, J Karácsony and S Biri for discussions. The help of T J Forgács, J Tóth, E Sárközi and Gy Császár in the construction of the experimental apparatus is gratefully acknowledged.

References

[1] Jonkers J, van de Sande M, Sola A, Gamero A and van der Mullen J 2003 *Plasma Sources Sci. Technol.* **12** 30
[2] Jonkers J, van de Sande M, Sola A, Gamero A, Rodero A and van der Mullen J 2003 *Plasma Sources Sci. Technol.* **12** 464
[3] Collins C B, Cunningham A J and Stockton M 1974 *Appl. Phys. Lett.* **25** 344
[4] Rothe D E and Tan K O 1977 *Appl. Phys. Lett.* **30** 152
[5] Hill P C and Herman P R 1993 *Phys. Rev.* A **47** 4837
[6] Hagelaar G J M, Kroesen G M W, van Slooten U and Schreuders H 2000 *J. Appl. Phys.* **88** 2252
[7] Petrov G M *et al* 2000 *Plasma Chem. Plasma Process.* **20** 183
[8] Peres I, Alves L L, Margot J, Sadi T, Ferreira C M, Tran K C and Hubert J 1999 *Plasma Chem. Plasma Process.* **19** 467
[9] Surendra M, Graves D B and Jellum G M 1990 *Phys. Rev.* A **41** 1112
[10] Boeuf J P and Pitchford L C 1991 *IEEE Trans. Plasma Sci.* **19** 286
[11] Fiala A, Pitchford L C and Boeuf J P 1994 *Phys. Rev.* E **49** 5607
[12] Donkó Z 1998 *Phys. Rev.* E **57** 7126
[13] Pedoussat C 1999 *PhD Thesis* Université Paul Sabatier
[14] Baguer N, Bogaerts A and Gijbels R 2003 *J. Appl. Phys.* **94** 2212
[15] Chen F F 1965 *Plasma Diagnostic Techniques* ed R H Huddestone and S H Leonard (New York: Academic) p 113
[16] Griem H R 1963 *Phys. Rev.* **131** 1170
[17] Den Hartog E A, O'Brian T R and Lawler J E 1989 *Phys. Rev. Lett.* **62** 1500
[18] Arslanbekov R R and Kudryavtsev A A 1998 *Phys. Rev.* E **58** 6539
[19] Bogaerts A, Quentmeier A, Jakubowski N and Gijbels R 1995 *Spectrochim. Acta* B **50** 1337
[20] Angstadt A D, Whelan J and Hess K R 1993 *Microchem. J.* **47** 206
[21] Ohsawa A, Ohuchi M and Kubota T 1991 *Meas. Sci. Technol.* **2** 801
[22] Gamez G, Bogaerts A, Andrade F and Hieftje G M 2004 *Spectrochim. Acta* B **59** 435
[23] Warner B E 1979 *PhD Thesis* University of Colorado
[24] Leigh B J 1999 *PhD Thesis* Monash University
[25] Bánó G, Szalai L, Horváth P, Kutasi K, Donkó Z, Rózsa K and Adamowicz T M 2002 *J. Appl. Phys.* **92** 6372
[26] Kutasi K, Hartmann P and Donkó Z 2001 *J. Phys. D: Appl. Phys.* **34** 3368
[27] Morgan W L, Boeuf J P and Pitchford L C 1998 *Siglo Data base, CPAT and Kinema Software* http://www.csn.net/siglo
[28] Hornbeck J A and Molnar J P 1951 *Phys. Rev.* **84** 621
[29] Deloche R, Monchicourt P, Cheret M and Lambert F 1976 *Phys. Rev.* A **13** 1140
[30] Ichikawa Y and Teii S 1980 *J. Phys. D: Appl. Phys.* **13** 2031
[31] Alves L L, Gousset G and Ferreira C M 1992 *J. Phys. D: Appl. Phys.* **25** 1713
[32] Donkó Z 2001 *Phys. Rev.* E **64** 026401
[33] Marić D, Kutasi K, Malović G, Donkó Z and Petrović Z Lj 2002 *Eur. Phys. J.* D **21** 73
[34] Bogaerts A and Gijbels R 2002 *Plasma Sources Sci. Technol.* **11** 27
[35] Nikitovic Z, Malovic G, Strinic A and Petrovic Z 2003 *Bull. Am. Phys. Soc.* **48** 30
[36] Phelps A V and Petrović Z Lj 1999 *Plasma Sources Sci. Technol.* **8** R21
[37] Phelps A V 1960 *Phys. Rev.* **117** 619
[38] Hagstrum H G 1953 *Phys. Rev.* **91** 543
[39] Kutasi K and Donkó Z 2000 *J. Phys. D: Appl. Phys.* **33** 1081
[40] Sosov Y and Theodosiou C E 2004 *J. Appl. Phys.* **95** 4385
[41] Bouef J P and Pitchford L C 1995 *J. Phys. D: Appl. Phys.* **28** 2083